Proceedings of the 28th IEEE
EMBS Annual International Conference
New York City, USA, Aug 30-Sept 3, 2006

Segmentation of 4D Cardiac Images: Investigation on Statistical Shape Models

Markus S. Renno, Yan Shang, James Sweeney, and Olaf Dössel, *Member, IEEE*

Abstract— **The purpose of this research was two-fold: (1) to investigate the properties of statistical shape models constructed from manually segmented cardiac ventricular chambers to confirm the validity of an automatic 4-dimensional (4D) segmentation model that uses Gradient Vector Flow (GVF) images of the original data and (2) to develop software to further automate the steps necessary in active shape model (ASM) training. These goals were achieved by first constructing ASMs from manually segmented ventricular models by allowing the user to cite entire datasets for processing using a GVF-based landmarking procedure and Principal Component Analysis (PCA) to construct the statistical shape model. The statistical shape model of one dataset was used to regulate the segmentation of another dataset according to its GVF, and these results were then analyzed and found to accurately represent the original cardiac data when compared to the manual segmentation results as the golden standard.**

I. Introduction

MANY modern medical imaging applications require existing segmented 4D surface shape models [1]. Therefore, there is a need for a fast, accurate, and automatic segmentation procedure of 4D medical data. This research aims to validate and build on such an automatic segmentation method that uses ASMs to regulate the segmentation of the human left ventricle using the GVF of the medical imaging data. This paper begins with a discussion on manual segmentation, followed by the presentation of the process of ASM training, reconstruction, and automatic segmentation.

II. Image Data

There were altogether three 4D cardiac MRI sequences from healthy volunteers. Table 1 gives the balanced FFE sequence (TrueFISP) acquired image data parameters.

Manuscript received April 24, 2006. This work was supported in part by the Barrett Honors College and the Fulton Undergraduate Research Initiatives Program at Arizona State University.

M. S. Renno is an undergraduate with the Harrington Department of Bioengineering at Arizona State University, Tempe, AZ 85281, USA (phone: 480-452-2272; e-mail: markus.renno@asu.edu).

Y. Shang was completing her doctorate at the Institute für Biomedizinische Technik, Universität Karlsruhe, Karlsruhe, Germany. She is now with the Department of Electronic Engineering, Tsinghua University, Beijing, P. R. China (e-mail: yan.shang@ibt.uni-karlsruhe.de).

J. Sweeney is with the Harrington Department of Bioengineering, Arizona State University, Tempe, AZ 85281, USA (e-mail: james.sweeney@asu.edu).

O. Dössel is with the Institute für Biomedizinische Technik, Universität Karlsruhe, Karlsruhe, Germany (e-mail: olaf.doessel@ibt.uni-karlsruhe.de).

The image orientation for vol01 and vol02 was transverse, and for vol03 was transverse rotated by 30° around the right-left axis of the patient. The first necessary step was converting the format of the original MRI cardiac dataset to kaLattice format, the internal 3D image format at the Institut für Biomedizinische Technik (IBT). First, the header information was processed to obtain the size and position of the real image data. Because the original 4D datasets were divided into files that contain images for one slice at all heart phases, the slice data of one phase from all the files had to be combined into 3D datasets to get the desired 3D heart image data for different phases. Finally, the header information for kaLattice and the image data had to be filled correctly. Using a 2D visualization tool MultiView the converted results could be checked slice by slice at each heart phase.

The original image data type was float and, because the human eye can usually perceive gray differences of 256 grades, could be converted to char, reducing the gray level images to 256 grades, decreasing storage need, and increasing processing speed.

Next, the original anisotropic image data needed to be transformed into isotropic lattice data. First, the transform matrix of the original data was set. The isotropic lattice size was then calculated, and the anisotropic lattice was transformed into the isotropic lattice of new size using linear interpolation. Noise in the original image data was reduced by non-linear filtering methods, which proved most suitable for de-noising while keeping the edge information. The converted isotropic 3D Lattice data for slice 36 at two different heart cycle phases of vol01 are shown in Fig. 1.

TABLE I
ORIGINAL AND PROCESSED IMAGE PARAMETERS

Data Set	vol01/02	vol03
FOV [mm]	350x350	370x370
Voxel matrix	256x256	256x256
(real) resolution [mm]	1.82x1.37	1.45x1.45
(reconstructed) resolution [mm]	1.37x1.37	1.45x1.45
slices	32	19
slice thickness [mm]	5	5
cardiac frequency [bpm]	60/55	80
heart phases	25	18

III. Manual Segmentation

Manual segmentation of the 3D phase images into triangle mesh models was carried out directly in the 3D image, which allowed interactive construction of the heart surfaces [2], [3]. First, an initial spherical contour was constructed; this contour was then deformed under the control of the mouse movement in the 2D slice view in MultiView. The

movement of an element caused the movement of adjacent regions, as controlled by a radial basis function transformation and could then be observed using a 3D visualization tool View3D.

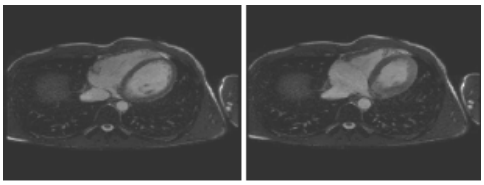

Fig. 1. Isotropic MRI images at same slice for vol01. Phase 1 (left) and Phase 14 (right) are shown here.

IV. STATISTICAL SHAPE MODEL CONSTRUCTION

The ASM training for application to automatic segmentation required multiple steps to create an effective model. The tasks included calculating the GVF of the manually segmented models, landmarking the triangle mesh files, and finally, conducting PCA of the landmarked files [7].

A. Calculating the Gradient Vector Flow

The first task in creating the statistical shape model was calculating the GVF diagrams of the cropped edge maps for each set of planes in the x, y, and z directions. GVF diagrams indicate the component gradient of the lattice by the intensity of the gray value [8], [9]. Two examples of GVF diagrams are shown at same slice in Fig. 2, where on screen red indicated the gradient in the x direction, green indicated the gradient in the y direction, and blue indicated the gradient in the z direction.

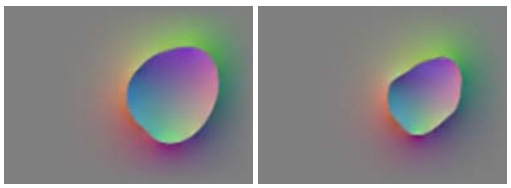

Fig. 2. GVF images for vol01 Phase 1 epicardium (left) and endocardium (right).

B. Landmarking the Triangle Meshes

The next step in training the ASM was establishing point to point associations between the manually segmented triangle mesh files. This was accomplished through a landmarking procedure that first required the resolution of the lattice matrices to be in unit form [10]. Thus, a brief conversion program was developed to prepare the edge map lattice files for template generation, the first step in the landmarking process.

Next, the templates for deformation according to the GVF of each other phase were created with fewer triangles than the original manually segmented models using open the source software MarchingCubeDeci.tcl, which reduces the triangle mesh resolution by the marching cube method [11]. This resolution reduction was necessary to accelerate the processor-intensive PCA to follow. To investigate the effectiveness of different template resolutions in the automatic segmentation to follow, 25, 50, 100, and 200 iterations of the decimation process were conducted. Also, to determine the effect of varying the phase used as a template, the systole, diastole, and one phase in between were used, resulting in a total of 24 templates for each data set: 4 resolutions, 3 phases, and 2 edge maps (left ventricle endocardium and epicardium). The resulting templates were then converted to the internal TriMesh format.

The landmarking procedure entailed deforming the triangle points in the template mesh files according to the GVF of the other phases to establish point to point relationships of the vertex position vectors of each phase. Software was developed to automate the multiple iterations of the landmarking procedure for entire datasets. The deformation of the template from phase 1 with 50 decimations to GVF of phase 16 of vol01 is shown in Fig. 3.

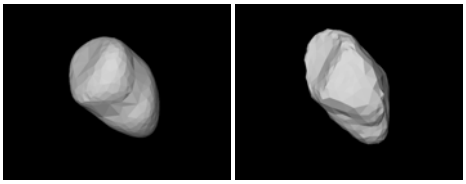

Fig. 3. Landmarking by deforming the template triangle mesh (left) to the resultant triangle mesh (right) according to its GVF.

C. Principal Component Analysis

Following the landmarking procedure, PCA was conducted to calculate the triangle mesh average and variance along different model deformation vectors or axes of the landmarked 4D data set. Specifically, PCA calculates the eigenvectors in which direction the active shape model average is allowed to deform in automatic segmentation of other ventricular datasets, and each eigenvector's corresponding eigenvalue defines the variance in the direction of the eigenvector [12]. The variance of the surface shape models caused by the first five PCA eigenvalues is illustrated in Fig. 4.

Upon visual inspection of the variance images, the first and largest eigenvalue appears to govern the 3D size, thus regulating the general variance in the time dimension during automatic segmentation. Eigenvalue two (x) tends to regulate the position along the ventricular long axis toward the left atrium and extension of the length of the ventricle in the same direction. Eigenvalues three and four (y and z) appear to govern deformation away from the heart perpendicular to each other and in the plane normal to the long axis, i.e. perpendicular to the axial deformation of eigenvector two. The greatest four eigenvalues can therefore be said to regulate the temporal and spatial variance in the primary four dimensions of the dataset: time, x, y, and z. Eigenvalues five and above control the fine tuning of the model deformation in composite directions through all three primary axes. These observations become especially significant in the context of the reconstruction parameters discussed next.

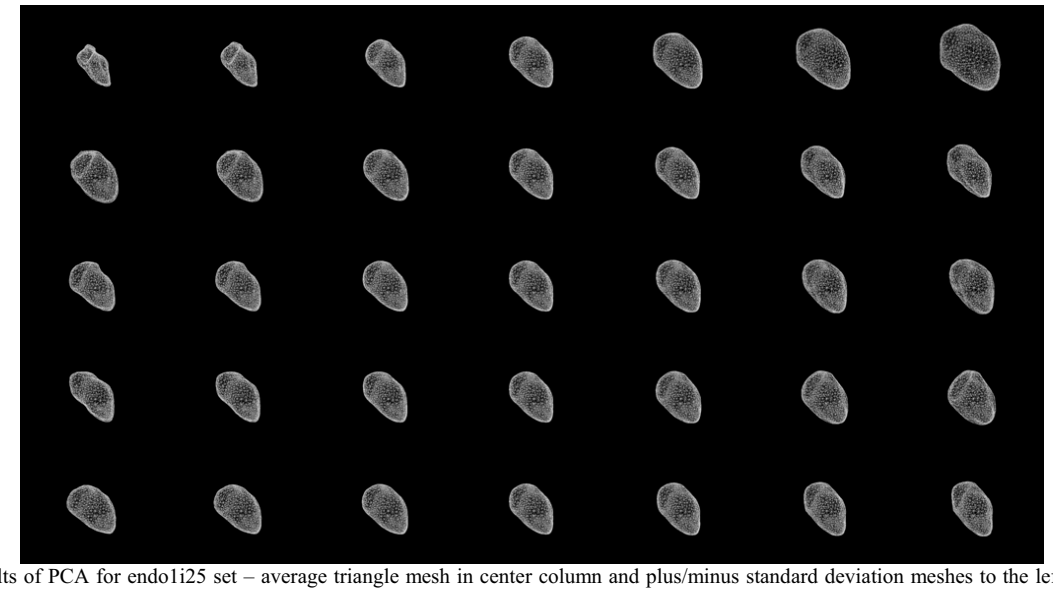

Fig. 4. Results of PCA for endo1i25 set – average triangle mesh in center column and plus/minus standard deviation meshes to the left and right for eigenvalues one through five in corresponding rows.

V. RECONSTRUCTION PARAMETER ANALYSIS

With the statistical shape model complete, the landmarked triangle meshes of the original manually segmented results were reconstructed using the PCA results to determine the characteristics of the reconstruction parameters, i.e. the characteristic magnitudes necessary to recreate a phase from the PCA average when multiplied by each eigenvalue's respective eigenvector. The reconstruction automation software creates reconstructed triangle meshes, and prints the reconstruction parameters for each eigenvalue in a list files for extraction and graphing as functions of time, i.e. phase. These results were then used to compare results between phase and resolution used in template creation for the landmarking procedure.

In general, the reconstruction parameters with respect to time exhibited similar shapes with magnitude differences. This variation of the magnitudes tended to be more significant with regard to resolution differences than template phase differences. Also, certain templates and resolutions had negative magnification constants, causing the curves to be flipped with respect to the others. This simply implies that the eigenvector of that eigenvalue set was oriented in the opposite direction, though the effectiveness of the PCA model in automatic segmentation is actually unaffected by the eigenvector orientation.

It is furthermore especially interesting to note the similarities between the graphs for the first eigenvalue and the volumetric series of the original manually segmented results as shown in Fig. 5. It was observed that the model as a function of time was the average PCA model plus the summation of the reconstruction parameters multiplied by their respective eigenvectors. This conclusion has great implications for the possibility of 4D shape interpolation from 3D data. For example, given a low resolution 4D dataset and a high resolution 3D model of the same heart, it would be possible to extract the reconstruction parameters of the statistical shape model of the 4D data for application to deformation of the high resolution 3D model, resulting in a high resolution 4D model.

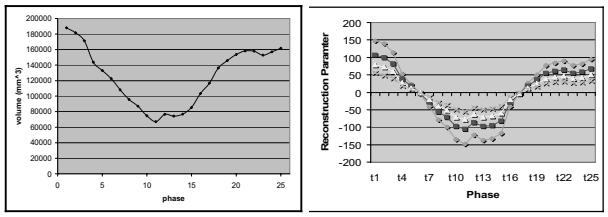

Fig. 5. Comparison of volumetric series for manual segmentation (left) and reconstruction parameters for vol01 eigenvalue 1 (right).

VI. AUTOMATIC SEGMENTATION

Having investigated the characteristics of the statistical shape model through its PCA results and reconstruction parameters, the ASMs of different resolutions of the vol02 endocardium were then applied to regulate automatic segmentation of the original cropped 4D dataset of vol01 through deformation of the ASMs toward the GVF of vol01 [13, 14]. The first step in the process was calculating the GVF diagrams of the cropped vol01 lattices. Then, the GVF forces were applied to the PCA results of vol02, for which 25, 50, 100, and 200 decimations had been applied to phase one for landmarking template generation. Noting the decreasingly accurate results with decreasing resolution, i.e. increasing decimations, the automatic results using the 100- and 200-decimation PCA model were discarded, and a damped PCA restriction was applied to automatically segment the data with the 100-decimation PCA model, thereby giving the GVF of vol01 greater influence on the automatic segmentation.

The active shape model application to 4D cardiac MRI data was validated by visual inspection of the triangle meshes superimposed on their respective lattices while

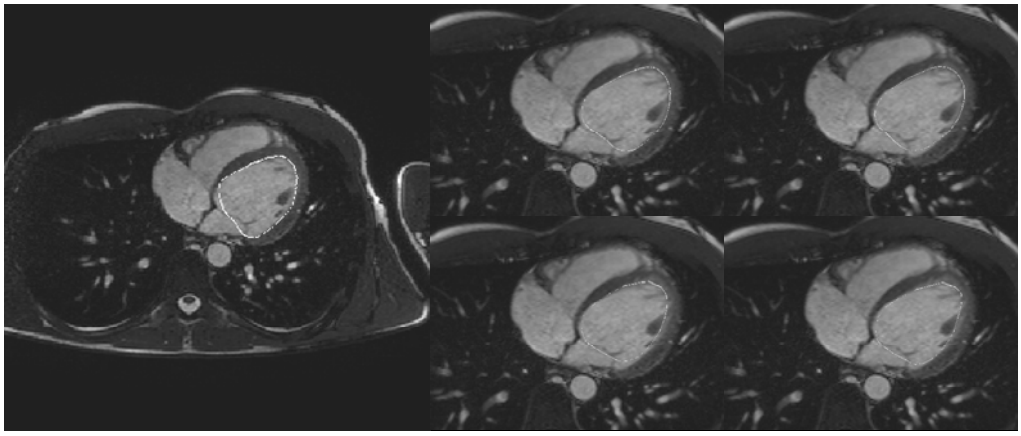

Fig. 6. Comparison of manual segmentation (left) with automatic segmentation from PCA models derived from landmarked templates with 25 (top center), 50 (top right), 100 (bottom center) decimations, and lesser PCA restriction for the template with 100 decimations (bottom right) at same slice.

comparing to the manual segmentation results. See Fig. 6 for a comparison of results between resolutions at same slice. The lower resolution statistical shape models were not as accurate as the high resolution models when used in automatic segmentation. The results from the segmentation of vol01 using the 25- and 50-decimation PCA models of vol02 were found to be very acceptable and should therefore be replicated with more 4D datasets for further application and validation. The results from the segmentation using the 100- and 200-decimation PCA models were not acceptable and better resembled the vol02 model than the vol01 model it was supposed to create. The use of PCA damping for automatic segmentation using the 100-decimation PCA model improved the automatic segmentation with respect to the original 100-decimation segmentation but nevertheless caused problems in regions where the vol02 statistical shape model is supposed to negate the vol01 GVF force effects, especially in the left atrium-left ventricle edge region and the papillary muscle region. Despite the failure of the model for lower resolution ASMs however, the subjective visual review effectively confirmed the automatic segmentation results for high resolution models.

VII. CONCLUSION

The need for faster, more efficient, yet still accurate cardiac segmentation models is becoming more and more necessary, especially in areas of state of the art research. Manually segmenting three left ventricles was a very tedious and time-consuming process that, though relatively easy to do with the given tools, can not practically be applied in patient treatment modeling. The creation of ASMs can now be achieved through fairly automated software and requires far less user interaction than previously. The extraction of the reconstruction parameters demonstrated the relationship of the parameters to the models from which the ASMs were trained: the reconstruction parameters indicate the magnitude of motion in the direction of each eigenvalue's eigenvectors. These parameters could therefore be applied to interpolate 4D datasets from a few 3D models. Furthermore, it was demonstrated that the automatic segmentation method proposed can accurately create 4D models of MRI, certainly as well as other, datasets.

REFERENCES

[1] A Frangi, et al. "Three-Dimensional Modeling for Functional Analysis of Cardiac Images: A Review." *IEEE Transactions on Medical Imaging, vol. 20, no. 1.* January, 2001.

[2] Nils Busch. F. B. Sachse and C. D. Werner, eds. "Segmentation klinischer vierdimensionaler magnetresonanztomographischer Aufnahmen mittels Aktiver Kontur Modelle und haptischer Interaktion." *Institut für Biomedizinische Technik, Universität Karlsruhe,* Diploma Thesis, 1998.

[3] Peter Zerfass. F. B. Sachse and C. D. Werner, eds. "Interaktive Deformation von Dreiecksnetzen zur Segmentation tomographischer Aufnahmen." *Institut für Biomedizinische Technik, Universität Karlsruhe,* Diploma Thesis, 2000.

[4] S. Silbernagl and A. Despopoulos. *Taschenatlas der Physiologie.* Georg Thieme Verlag, Stuttgart/New York: 2001.

[5] C. H. Lorenz, et al. "Normal human right and left ventricular mass, systolic function, and gender differences by cine magnetic resonance imaging." *Journal of Cardiovascular Magnetic Resonance, vol. 1, no. 1.* January, 1999: pp. 7-21.

[6] C. Vuille and A. E. Weyman. "Left ventricle I: General considerations, assessment of chamber size and function." *Principles and Practice of Echocardiography, 2nd ed, A. E. Weyman, Ed.* Lea and Febiger Philadelphia, PA: 1994.

[7] T.F. Cootes, et al. "Active Shape Models – Their Training and Application." *Computer Vision and Image Understanding, vol. 61, no. 1.* January, 1995: pp. 38-59.

[8] C Xu and J Prince. "Snakes, Shapes, and Gradient Vector Flow." *IEEE Transactions on Medical Image Processing, vol. 7, no. 3.* March, 1998.

[9] Rong Liu. Y. Shang and F. B. Sachse, eds. "3D Active Surfaces for Segmentation of Medical Image Data: Assessment of Different Image Forces." *Institut für Biomedizinische Technik, Universität Karlsruhe,* Diploma Thesis, 2003.

[10] Y Shang and O Dössel. "Landmarking Method of 3D Surface Models for Construction of 4D Cardiac Shape Model." *Biomedizinische Technik, vol. 48-1.* September, 2003: pp 124-125.

[11] Kitware, Inc. (n.d.) *The Visualization Toolkit*. Retrieved July 27, 2005, from http://www.vtk.org.

[12] R. A. Johnson and D. W. Wichern. *Multivariate Statistics, A Practical Approach*. Chapman & Hall, London/New York: 1998.

[13] Y. Shang and O. Dössel. "Statistical 3D Shape-Model Guided Segmentation of Cardiac Images." *Proceedings Computers in Cardiology*. Chicago: October, 2004.

[14] Y. Shang and O. Dössel. "Construction of Cardiac Anatomical Models Using Deformable Model Methods." *Bildverarbeitung für die Medizin 2004*. Berlin: February, 2004.